Computation of a Turbulent Natural Convection in a Rectangular Cavity with the Low-Reynolds-Number Differential Stress and Flux Model

Seok-Ki Choi*, Eui-Kwang Kim, Myung-Hwan Wi, Seong-O Kim
Korea Atomic Energy Research Institute,
Fluid System Engineering Division,
150 Deokjin-dong, Yuseong-gu, Daejeon, 305-353, Korea

A numerical study of a natural convection in a rectangular cavity with the low-Reynolds-number differential stress and flux model is presented. The primary emphasis of the study is placed on the investigation of the accuracy and numerical stability of the low-Reynolds-number differential stress and flux model for a natural convection problem. The turbulence model considered in the study is that developed by Peeters and Henkes (1992) and further refined by Dol and Hanjalic (2001), and this model is applied to the prediction of a natural convection in a rectangular cavity together with the two-layer model, the shear stress transport model and the time-scale bound $\overline{v^2}-f$ model, all with an algebraic heat flux model. The computed results are compared with the experimental data commonly used for the validation of the turbulence models. It is shown that the low-Reynolds-number differential stress and flux model predicts well the mean velocity and temperature, the vertical velocity fluctuation, the Reynolds shear stress, the horizontal turbulent heat flux, the local Nusselt number and the wall shear stress, but slightly under-predicts the vertical turbulent heat flux. The performance of the $\overline{v^2}-f$ model is comparable to that of the low-Reynolds-number differential stress and flux model except for the over-prediction of the horizontal turbulent heat flux. The two-layer model predicts poorly the mean vertical velocity component and under-predicts the wall shear stress and the local Nusselt number. The shear stress transport model predicts well the mean velocity, but the general performance of the shear stress transport model is nearly the same as that of the two-layer model, under-predicting the local Nusselt number and the turbulent quantities.

Key Words : Turbulent Natural Convection, Two-Layer Model, Shear Stress Transport Model, $\overline{v^2}-f$ Model, Low-Reynolds-Number Differential Stress And Flux Model

Nomenclature

g_i : Gravitational acceleration
G_k : Buoyancy generation term
H : Height of the cavity
h : Heat transfer coefficient
k : Turbulent kinetic energy
k_f : Conductivity of fluid
L : Width of the cavity
n_i : i-th component of normal vector at the wall
Nu : Nusselt number
p : Pressure
P_k : Generation term of turbulent kinetic energy
P_θ : Generation term of temperature variance
Pr : Prandtl number
Pr_θ : Turbulent Prandtl number
Ra : Rayleigh number
R_T : Turbulent Reynolds number $\left(=\frac{\rho k^2}{\mu\varepsilon}\right)$

* Corresponding Author,
E-mail : skchoi@kaeri.re.kr
TEL : +82-42-868-2993; **FAX** : +82-42-868-8363
Korea Atomic Energy Research Institute, Fluid System Engineering Division, 150 Deokjin-dong, Yuseong-gu, Daejeon, 305-353, Korea (Manuscript **Received** September 16, 2003; **Revised** June 8, 2004)

t : Time
T : Time scale
U_i : Cartesian velocity components
$\overline{u_i u_j}$: Reynolds stresses
U_τ : Wall friction velocity $\left(=\left(\frac{\mu}{\rho}\left|\frac{\partial U_P}{\partial x_n}\right|_w\right)^{1/2}\right)$
x_i : Cartesian Coordinates
x_n : Normal distance from the wall
x_n^+ : Dimensionless normal distance from the wall $\left(=\frac{\rho U_\tau x_n}{\mu}\right)$

Greeks

β : Gas expansion coefficient
Δn : Normal distance from the wall
ε : Dissipation rate of turbulent kinetic energy
ε_θ : Dissipation rate of temperature fluctuation
μ : Dynamic viscosity
μ_{ij}^M : Pseudo eddy-viscosity for momentum equations
μ_j^T : Pseudo eddy-viscosity for energy equation
μ_T : Turbulent eddy viscosity
ν : Kinematic viscosity
ρ : Density
Θ : Temperature
$\overline{\theta u_i}$: Turbulent heat fluxes
$\overline{\theta^2}$: Temperature variance

Subscripts

H : Pertaining to hot wall
ε : Pertaining to dissipation rate of turbulent kinetic energy
θ : Pertaining to temperature

Superscripts

$N-1$: Pertaining to previous iteration level
M : Pertaining to momentum equation
T : Pertaining to energy equation

1. Introduction

Accurate prediction of a natural convection is very important for investigating the fluid flow and heat transfer in various engineering applications such as a reactor vessel auxiliary cooling system in a liquid metal reactor, solar collectors and electronic equipment cooling. The natural convection also plays a very important role in thermal stratification such as that in the upper plenum of a liquid metal reactor during the scram condition. Despite its importance in practical engineering problems, turbulent natural convection has received attention only from a few researchers. There exist little experimental data to validate the computer codes, mainly due to experimental difficulties. It is still difficult to measure the low velocity and to achieve the ideal adiabatic condition. The experimental data by Tsuji and Nagano (1987) for a heated vertical plate, by Betts and Bokhari (2000) for a tall cavity, by King (1989) and Cheesewright et al. (1986) for a rectangular cavity, and by Tian and Karayiannis (2000) and Ampofo and Karayiannis (2003) for a square cavity are examples of experimental data which have been used by many authors to test turbulence models or to validate their computer codes. The LES (Large Eddy Simulation) by Peng and Davidson (2001) for a natural convection in a square cavity for the experiment by Tian and Karayiannis (2000) and the DNS (Direct Numerical Simulation) by Boudjemadi et al. (1997) and by Versteegh and Nieuwstadt (1998) are examples of the LES and DNS studies reported in the literatures. Most works in the literature employ the RANS (Reynolds Averaged Navier-Stokes) equation approach. In the RANS equation approach, the choice of a turbulence model is crucial, as it directly affects the accuracy of the solutions. However, the turbulence modeling of a natural convection is still difficult and the rationale for the difficulties is well explained in Hanjalic (2002) and Dol et al. (1997).

One of the difficulties of the computation of a natural convection by the conventional $k-\varepsilon$ model is the validity of the wall function method, which is based on the local equilibrium logarithmic velocity and temperature assumptions. The logarithmic wall functions were originally derived for the forced-convection flows and do not hold for natural convection boundary layers. Due to this problem, most previous authors used the low-Reynolds-number turbulence models for a computation of the natural convection problems, for example, Henkes et al. (1991). The other difficulty in predicting the turbulent natural convection is the treatment of the turbulent heat

fluxes. If one does not use the differential flux model, a proper way of treating the turbulent fluxes should be sought. Ince and Launder (1989) explained that the simple gradient formulation is not a proper way of treating the turbulent heat fluxes and proposed a generalized gradient formulation. However, Kenjeres (1998) has shown that the algebraic flux model developed by Hanjalic and Kenjeres (1995) results in better solutions than the generalized gradient formulation for a turbulent natural convection in a rectangular cavity. A good feature of the algebraic heat flux model developed by Hanjalic and Kenjeres (1995) is its simplicity, it requires only one additional solution of the transport equation for a temperature variance. The main difference between this model and the general gradient diffusion hypothesis proposed by Ince and Launder (1989) is the inclusion of the temperature variance term in the algebraic expression of the turbulent heat fluxes. The use of this model is attractive due to its simplicity of implementation and high performance. This algebraic flux model (AFM hereafter) will be used in the present study for the computation of a natural convection in a rectangular cavity together with the two-layer model by Chen and Patel (1988), the shear stress transport model (SST hereafter) by Menter (1994) and the time-scale bound $\overline{v^2}-f$ (V2-f hereafter) model by Medic and Durbin (2002). During the course of the present study, we find that the performance of the AFM depends much on the constants in the algebraic expressions of the turbulent heat fluxes, and the optimal values of the constants differ for different turbulence models and flow conditions. In the present study a systematic numerical experiment is conducted to obtain the optimal values of the constants for all the models considered in the present study for the calculation of the experiment by King (1989) and Cheesewright et al. (1986) for a rectangular cavity.

It can be commonly accepted that the use of the second-moment closure may result in better solutions for a natural convection in enclosures, however, the second-moment modeling of a natural convection requires the modeling of various terms in the transport equations for the turbulent heat flux vector, the temperature variance and the dissipation rate of the temperature variance, and its use in practical engineering problems is still questionable due to its complexity and demand of high computer resources. For the force convection flows, Lai and So (1990), Shikazo and Kasagi (1996) and Shin et al. (1993) have developed the near-wall second moment closures. There are a few works for the near-wall second moment models for the turbulent natural convection flows. Dol and Hanjalic (2001) performed two and three dimensional calculations for the experiments conducted by Opstelten (1994) and Dol et al. (2000) using the second-moment closure by Peeters and Henkes (1992), however, a limited success is reported although they showed that the second moment closures predict better than the conventional low-Reynolds-number $k-\varepsilon$ model. It is not clearly understood whether their limited success is due to a turbulence modeling problem or others, such as experimental or numerical errors. They do not show the results for the important heat transfer parameters such as the local Nusselt number and the turbulent heat fluxes. In the present study we perform two-dimensional calculations using the same turbulence model, but for a different experiment by King (1989) and Cheesewright et al. (1986) for a rectangular cavity. The computed results by the two-layer model, the SST model and the V2-f model are also included for comparison purposes. The results of this kind of study may contribute to understanding the success and limit of the current second-moment closures for a turbulent natural convection in enclosures.

In the following chapters, first a brief outline of the numerical issues for using the second-moment closures is presented. Then, the computed results for four different turbulence models are presented, followed by the conclusions drawn from the present study

2. Mathematical Formulation

2.1 Governing equations

The Reynolds averaged governing equations for the mass conservation, momentum conservati-

on, energy conservation and the transport equations for the turbulent quantities in the low-Reynolds-number differential stress and flux model by Peeters and Henkes (1992) (SMC-PH hereafter) and further refined by Dol and Hanjalic (2001), can be written as follows;

$$\frac{D}{Dt}(\rho)=0 \tag{1}$$

$$\frac{D}{Dt}(\rho U_i)=-\frac{\partial p}{\partial x_i}+\frac{\partial}{\partial x_j}\left(\mu\frac{\partial U_i}{\partial x_j}-\rho\overline{u_iu_j}\right)-\rho\beta g_i(\Theta-\Theta_{ref}) \tag{2}$$

$$\frac{D}{Dt}(\rho\Theta)=\frac{\partial}{\partial x_j}\left(\frac{\mu}{\mathrm{Pr}}\frac{\partial\Theta}{\partial x_j}-\rho\overline{\theta u_j}\right) \tag{3}$$

$$\frac{D}{Dt}(\rho\overline{u_iu_j})=\frac{\partial}{\partial x_k}\left[\left(\mu\delta_{kl}+C_s\rho\overline{u_ku_l}\frac{k}{\varepsilon}\right)\frac{\partial\overline{u_iu_j}}{\partial x_l}\right]+(P_{ij}+G_{ij}+\Phi_{ij}-\rho\varepsilon_{ij}+E_{ij}) \tag{4}$$

$$\frac{D}{Dt}(\rho\varepsilon)=\frac{\partial}{\partial x_k}\left[\left(\mu\delta_{kl}+C_\varepsilon\rho\overline{u_ku_l}\frac{k}{\varepsilon}\right)\frac{\partial\varepsilon}{\partial x_l}\right]+\frac{\varepsilon}{k}(C_{\varepsilon1}f_{\varepsilon1}(P_k+C_{\varepsilon3}G_k)-C_{\varepsilon2}\rho f_{\varepsilon2}\varepsilon)+E_\varepsilon \tag{5}$$

$$\frac{D}{Dt}(\rho\overline{\theta u_i})=\frac{\partial}{\partial x_k}\left[\left(\frac{1}{2}\left(\mu+\frac{\mu}{\mathrm{Pr}}\right)\delta_{kl}+C_{\theta u}\rho\overline{u_ku_l}\frac{k}{\varepsilon}\right)\frac{\partial\overline{\theta u_i}}{\partial x_l}\right]+(P^t_{i\theta}+P^m_{i\theta}+G_{i\theta}+\Phi_{i\theta}+E_{i\theta}) \tag{6}$$

$$\frac{D}{Dt}(\rho\overline{\theta^2})=\frac{\partial}{\partial x_k}\left[\left(\frac{\mu}{\mathrm{Pr}}\delta_{kl}+C_{\theta\theta}\rho\overline{u_ku_l}\frac{k}{\varepsilon}\right)\frac{\partial\overline{\theta^2}}{\partial x_l}\right]+(2P_\theta-2\rho\varepsilon_\theta+2E_\theta) \tag{7}$$

$$\frac{D}{Dt}(\rho\varepsilon_\theta)=\frac{\partial}{\partial x_k}\left[\left(\frac{\mu}{\mathrm{Pr}}\delta_{kl}+C_{\varepsilon\theta}\rho\overline{u_ku_l}\frac{k}{\varepsilon}\right)\frac{\partial\varepsilon_\theta}{\partial x_l}\right]+(C_{P1}P_\theta-C_{D1}\rho\varepsilon_\theta)\frac{\varepsilon_\theta}{\theta^2}+(C_{P2}P_k-C_{D2}\rho\varepsilon)\frac{\varepsilon_\theta}{k} \tag{8}$$

The definitions of the variables and the values of the constants in Eqs. (4)-(8) are given in the Appendix. The details of the two-layer, SST and V2-f models used in the present study are given in Choi (2003). When the time scale-bound two-layer model, which is given in Medic and Durbin (2002), is used, there exists a sharp variation near the peak region for the turbulent heat fluxes, thus the conventional two-layer model is used in the present study. It is noted that in the three turbulence models except for the SMC-PH model, the turbulent heat fluxes are calculated using the following assumption in the AFM by Hanjalic and Kenjeres (1995);

$$\overline{\theta u_i}=-\frac{T}{C_{T1}}\left(\overline{u_iu_k}\frac{\partial\Theta}{\partial x_k}+(1-C_{T2})\overline{\theta u_k}\frac{\partial U_i}{\partial x_k}+(1-C_{T3})\beta g_i\overline{\theta^2}\right) \tag{9}$$

where T is the time-scale defined differently for the different models and can be seen in Choi (2003). The constants in Eq. (9) are not universal and are used differently by authors, see Kenjeres (1998), Hanjalic (2002) and Kenjeres and Hanjalic and (1995). As explained before a numerical experiment is conducted to obtain the optimal values for all the models for the calculation of the test problem in the present study. The Reynolds stresses in Eq. (9) are calculated by the following simple gradient formula.

$$\overline{u_iu_j}=\frac{2}{3}k\delta_{ij}-\nu_T\left(\frac{\partial U_i}{\partial x_j}+\frac{\partial U_j}{\partial x_i}\right) \tag{10}$$

2.2 Boundary conditions

At the wall a no slip boundary condition is imposed for the velocity components, and the isothermal and adiabatic wall boundary conditions are imposed for the temperature. The Reynolds stresses, the turbulent heat fluxes and the temperature variance are zero at the wall. In the SMC-PH model the dissipation rate of the turbulent kinetic energy and the dissipation rate of the temperature fluctuation are also zero at the solid wall.

3. Numerical Method

The most important issues for preserving a numerical stability in using the second-moment closure may be the introduction of the pseudo eddy-viscosities in the momentum and energy equations. The non-staggered grid method is used in the present study, and the introduction of the pseudo eddy-viscosities in the non-staggered grid configuration is well documented in Lien and Leschziner (1991). A brief outline of it is presented here. The momentum and energy equations, Eq. (2) and Eq. (3), can be written in the following forms by introducing the pseudo eddy-viscosities.

$$\frac{D}{Dt}(\rho U_i)=-\frac{\partial p}{\partial x_i}+\frac{\partial}{\partial x_j}\left((\mu+\mu^{\mathrm{M}}_{ij})\frac{\partial U_i}{\partial x_j}\right)-\rho\beta g_i(\Theta-\Theta_{ref})-\frac{\partial}{\partial x_j}\left(\rho\overline{u_iu_j}+\mu^{\mathrm{M}}_{ij}\frac{\partial U_i}{\partial x_j}\right)^{N-1} \tag{11}$$

$$\frac{D}{Dt}(\rho\Theta)=\frac{\partial}{\partial x_j}\left(\left(\frac{\mu}{\mathrm{Pr}}+\mu_j^T\right)\frac{\partial\Theta}{\partial x_j}\right) -\frac{\partial}{\partial x_j}\left(\mu_j^T\frac{\partial\Theta}{\partial x_j}+\rho\overline{\theta u_j}\right)^{N-1} \quad (12)$$

where the pseudo eddy-viscosities are defined as follows ;

$$\mu_{ij}^M=\frac{2-\frac{4}{3}C_2+\frac{2}{3}C_2C_{w2}(4f_i+f_j)}{C_1+2C_{w1}f_i}\rho\frac{k}{\varepsilon}\overline{u_iu_j}\quad i=j \quad (13)$$

$$\mu_{ij}^M=\frac{1-C_2+\frac{3}{2}C_2C_{w2}(f_i+f_j)}{C_1+\frac{3}{2}C_{w1}(f_i+f_j)}\rho\frac{k}{\varepsilon}\overline{u_iu_j}\quad i\neq j \quad (14)$$

$$\mu_j^T=\frac{1}{C_{\theta1}(1+C_{\theta w}f_j)}\rho\frac{k}{\varepsilon}\overline{u_ju_j} \quad (15)$$

j : *no-sumination*

and

$$f_i=n_i^2\frac{k^{3/2}}{\varepsilon C_l\Delta n} \quad (16)$$

The superscript $N-1$ in Eqs. (11)-(12) denotes the previous iteration value calculated by a deferred correction method. It should be noted that the introduction of the pseudo eddy-viscosities depends on the turbulence model used and the pseudo eddy-viscosities introduced in Eqs. (13)-(15) which are based on the SMC-PH model. With the above introduction of the pseudo eddy-viscosities and a proper source term linearization, no numerical stability problems are encountered. When the conventional steady state solution method is used, a numerical oscillation occurs, thus the unsteady time marching technique is employed with a suitable time step, typically $\Delta t=0.1$ sec.

The turbulence models considered in the present study are implemented in the computer code especially designed for the evaluation of the turbulence models. The computer code employs the non-staggered grid arrangement and the SIMPLE algorithm (Patankar, 1980) for the pressure-velocity coupling. The second-order bounded HLPA scheme (Zhu, 1991), which is the same as the Van-Leer's CLAM (Van Leer, 1974) scheme, is used for treating the convection terms.

4. Test Problem

As explained before, the experimental data by Tsuji and Nagano (1987) for a heated vertical plate, by Betts and Bokhari (2000) for a tall cavity, by King (1989) and Cheesewright et al. (1986) for a rectangular cavity, and by Tian and Karayiannis (2000) and Ampofo and Karayiannis (2003) for a square cavity are the typical experimental data which have been used by many authors to test the turbulence models. It is shown that the natural convection in a heated vertical plate experimented by Tsuji and Nagano (1987) is rather accurately calculated by Launder and Sharma model (1974) with AFM (Kenjeres, 1998), by V2-f model (Tieszen et al., 1998) or by SMC-PH model (Peeters and Henkes, 1992). In a natural convection in a tall cavity with a 1:28.6 aspect ratio measured by Betts and Bokhari (2000) the two boundary layers near the heated and cooled walls interact and the center of the cavity is a region of a maximum turbulence. It is also shown that this kind of flow can be calculated well by the low-Reynolds-number turbulence model (Kenjeres, 1998) or by the two-layer model (Hsieh and Lien, 2004). In the experiment by Ampofo and Karayiannis (2003) for a natural convection in a square cavity the turbulence level is low and the boundary layers near the hot and cold vertical walls are very thin and most of the cavity is quiescent and thermally stratified. The top and bottom walls are the conducting walls to avoid the problem of an imperfect insulation. It is reported that it is very difficult to obtain the steady state converged solution if the usual low-Reynolds-number turbulence model is employed (Hsieh and Lien, 2004). Due to the weak turbulence of this experiment there exists a LES solution by Peng and Davidson (2001). An evaluation of the turbulence models for this experiment has been recently done by the present authors and will be reported elsewhere. So far the experiment of King (1989) and Cheesewright et al. (1986) for a natural convection in a rectangular cavity with a 1:5 aspect ratio has been the most widely used by many authors to test the

turbulence models, for example, Ince and Launder (1989), Davidson (1990), Kenjeres (1998), Choi et al. (2004) and many others. This experiment has a problem in that the upper wall is not sufficiently insulated and Ince and Launder (1995) showed that a better prediction can be made by taking into account the effects of the heat loss and three-dimensionality of the flow. The turbulence level of this experiment is higher than that of the experiment by Ampofo and Karayiannis (2003) and the LES solution for this problem is not yet reported in the literature. Within the present author's knowledge, two of the most successful computations so far are due to Kenjeres (1998) using the Launder and Sharma model (1974) and due to Choi et al. (2004) using the V2-f model, both with AFM, and nobody has reported the computed results using the second-moment turbulence model. In the present study a rather comprehensive evaluation of turbulence models for this problem is done by including the near-wall second-moment closure.

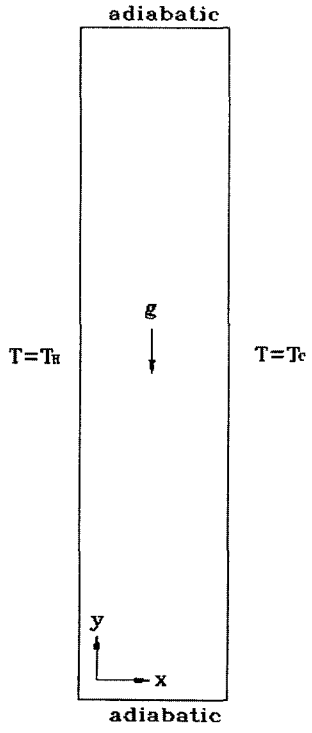

Fig. 1 A schematic picture of the 5:1 rectangular cavity.

The test problem considered in the present study is the natural convection of air in a rectangular cavity with an aspect ratio of 1:5 as shown in Fig. 1. The height of the cavity is $H=2.5m$, the width of the cavity is $L=0.5m$ and the temperature difference between the hot and cold walls is 45.8°K. The Rayleigh number based on the height of the cavity is $Ra=4.3\times10^{10}$ and the Prandtl number is Pr=0.7. King (1989) has carried out extensive measurements for this problem and the experimental data are reported in King (1989) and Cheesewright et al. (1986).

5. Results and Discussion

As explained before, the primary objective of the present study is the evaluation of the SMC-PH model for a natural convection in an enclosure. The numerical results by the two-layer, SST and V2-f models, all with the AFM, are also included for comparison. In order to investigate the grid dependency of the solution, calculations are performed using three different numerical grids, 62×92, 82×122 and 102×152. The numerical grids are generated using the method given in Henkes and Hoogendoorn (1995). Based on the calculation using the 102×152 grids, the first horizontal calculation point at the vertical center $(y/H=0.5)$ is located at $x^+=0.10\sim0.11$ depending on the turbulence models used. The interfaces between the two regions in the two-layer calculations are placed at a distance from wall where $[1-\exp(-R_x/62.5)]\approx0.95$ ($R_x=x\rho\sqrt{k}/\mu$), as is done by Medic and Durbin (2002). We found that the initial conditions affect the numerical stability for the V2-f and SMC-PH models calculations. The results of the two-layer model are used for the initial conditions for the SMC-PH and V2-f models computations.

Figures 2 (a)-(b) show the grid dependency of the solutions calculated by the SMC-PH model. We observe that the solutions using the 82×122 and 102×152 grids are grid independent indicating that the numerical grids used in the present study are fine enough, and we also observed that the solutions by the two-layer, SST and V2-f

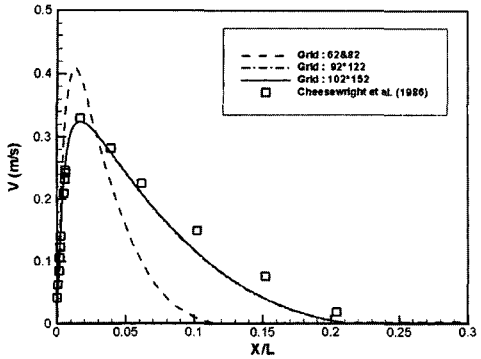

(a) Near wall vertical velocity profiles at $y/H=0.5$

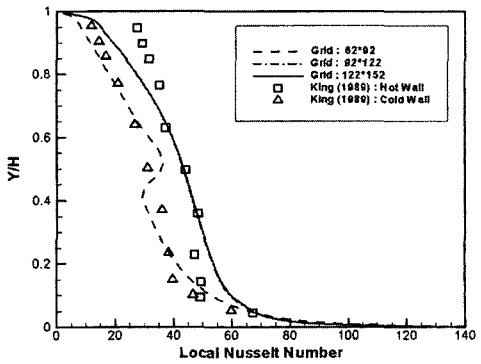

(b) Local Nusselt number profiles along the hot wall

Fig. 2 Grid dependency test

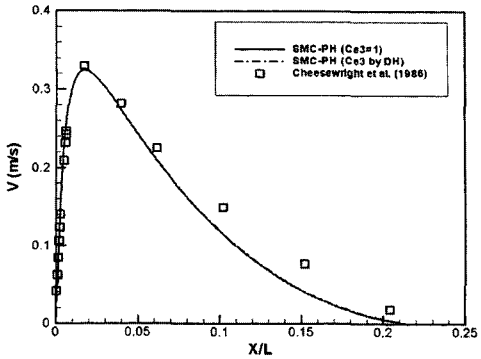

(a) Vertical velocity profiles at $y/H=0.5$ for experiment by Cheesewright et al. (1986).

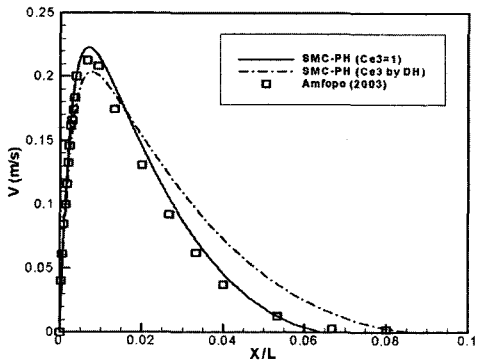

(b) Vertical velocity profiles at $y/H=0.5$ for experiment by Ampofo (2003).

Fig. 3 Effect of $C_{\varepsilon 3}$ on the solution for the SMC-PH model.

models are also grid independent, although they are not presented here. The solutions presented in the present study are those calculated using the finest 102×152 numerical grids.

Dol and Hanjalic (2001) (DH in Figs. 3 (a)-(b)) proposed the following new way of prescrisbing the $C_{\varepsilon 3}$ in the transport equation for the dissipation rate of the turbulence kinetic energy (see Appendix).

$$C_{\varepsilon 3}=\tanh|\cot(\theta)|, \quad \theta=\angle(U_i, g_i) \qquad (17)$$

This way leads to $C_{\varepsilon 3}\approx1$ in the vertical boundary layer and $C_{\varepsilon 3}\approx0$ in the horizontal flow, with a smooth transition in between. We have performed test calculations to investigate the validity of this assumption for the SMC-PH model. Figs. 3 (a)-(b) show that the treatment of $C_{\varepsilon 3}$ by Eq. (17) agrees well with the experimental data for a natural convection in a 1:5 rectangular cavity experimented by Cheesewright et al. (1986) while the vertical velocity component at the edge of the boundary layer deviates a lot from the experimental data for a natural convection in a square cavity experimented by and Ampofo and Karayiannis (2003). We can see that $C_{\varepsilon 3}=1$ is the right choice for the usual way done by Ince and Launder (1989), Choi et al. (2004) and many others. The reason why the treatment of $C_{\varepsilon 3}$ by Eq. (17) produces an accurate solution for a 1:5 rectangular cavity is that it leads to $C_{\varepsilon 3}\approx1$ in a nearly whole solution domain except for the region near the top and bottom walls.

Before going into a detailed comparison among the different turbulence models a systematic numerical experiment is conducted to obtain the optimal constants of the AFM, Eq. (9), for the turbulence models tested in the present study for the experiment conducted by King (1989) and Cheesewright et al. (1986). Figures 4-7 show the predicted vertical mean velocity and the vertical turbulent heat flux for different values of the con-

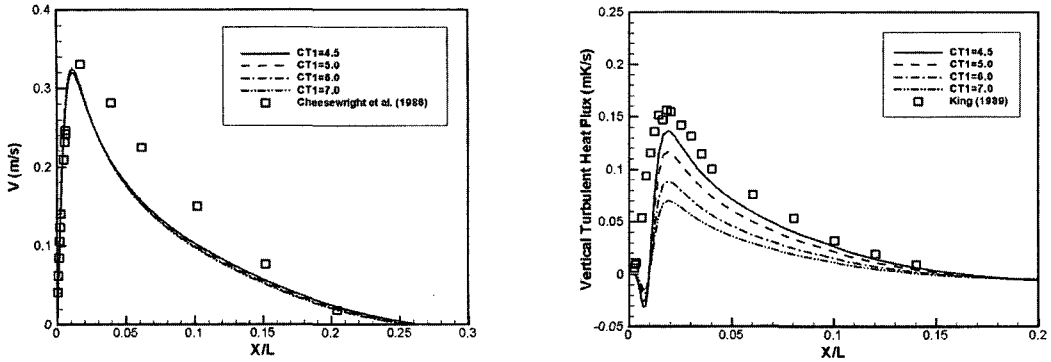

(a) Vertical velocity profiles at $y/H=0.5$ (b) Vertical turbulent heat flux profiles at $y/H=0.5$

Fig. 4 Effect of C_{T1} on the solution for the two-layer molel

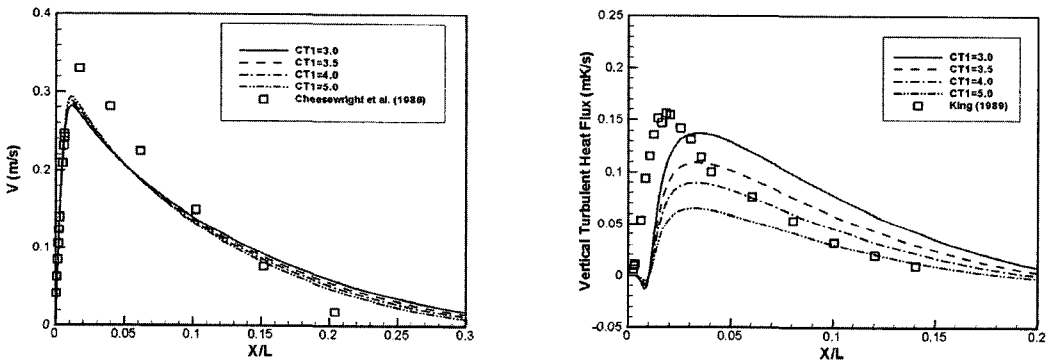

(a) Vertical velocity profiles at $y/H=0.5$ (b) Vertical turbulent heat flux profiles at $y/H=0.5$

Fig. 5 Effect of C_{T1} on the solution for the $k-\omega$ molel

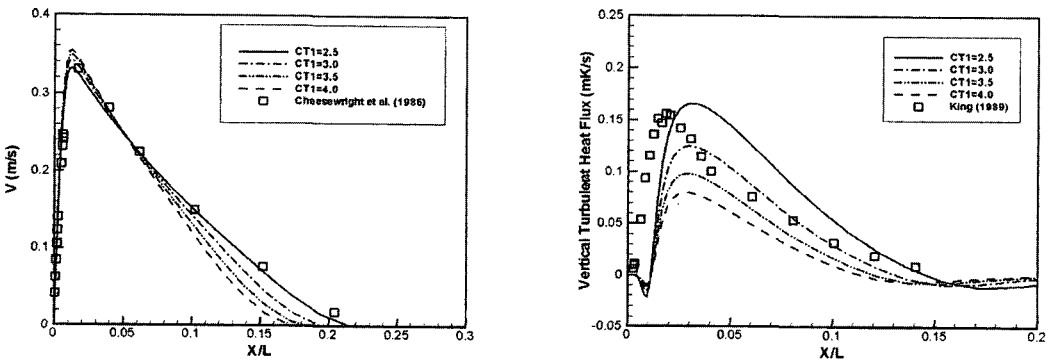

(a) Vertical velocity profiles at $y/H=0.5$ (b) Vertical turbulent heat flux profiles at $y/H=0.5$

Fig. 6 Effect of C_{T1} on the solution for the SST molel

stants in the AFM. We can observe that the solutions vary much with the constant and the optimal constants are different for different turbulence models. The optimal constants of the AFM for the experiment conducted by King (1989) and Cheesewright et al. (1986) are $C_{T1}=4.5$ for the two-layer model, $C_{T1}=4.0$ for the $k-\omega$ model, $C_{T1}=3.0$ for the SST model and $C_{T1}=7.0$ for the V2-f model.

In the initial stage of the present study the $k-\omega$ model was tested as shown in the Fig. 8 and it is found that the $k-\omega$ model produces very

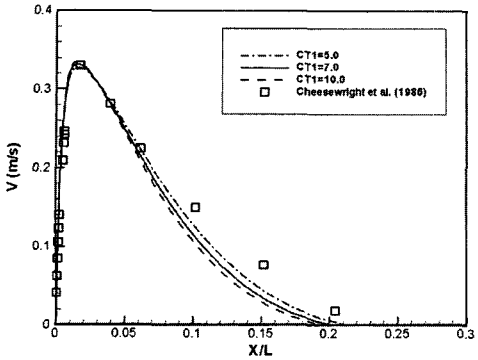

(a) Vertical velocity profiles at $y/H=0.5$

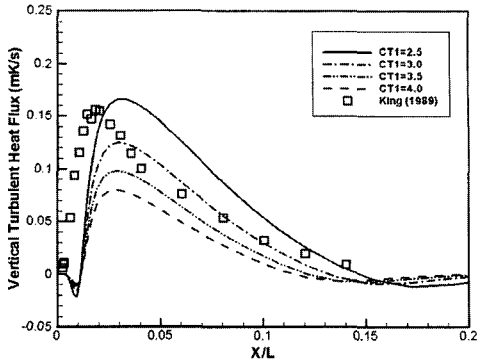

(b) Vertical turbulent heat flux profiles at $y/H=0.5$

Fig. 7 Effect of C_{T1} on the solution for the $\overline{v^2}-f$ molel.

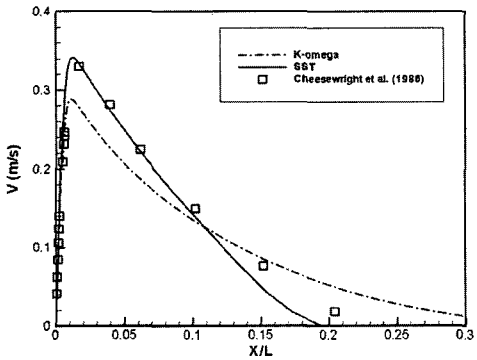

(a) Vertical velocity profiles at $y/H=0.5$

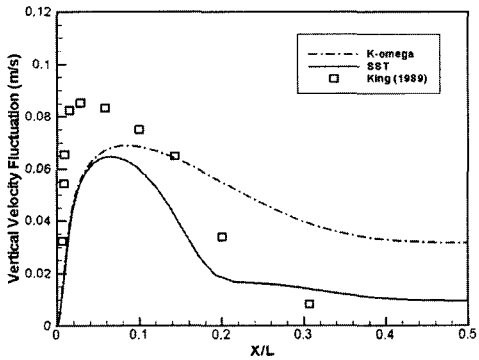

(b) Vertical turbulent heat flux profiles at $y/H=0.5$

Fig. 8 Comparison of performances of the $k-\omega$ molel and SST model.

diffusive solutions at the edge of the boundary layer, especially the vertical velocity fluctuation. This is a well known defect of the $k-\omega$ model and Menter (1994) developed the SST model to remove this problem. We can observe that the introduction of the SST model removes this strange behavior of the $k-\omega$ model at the edge of the boundary layer although the profile of the vertical velocity fluctuation is not smooth at that region. Due to this reason the SST model is adopted in the present study instead of the $k-\omega$ model

Figure 9 and Fig. 10 show the streamlines and isotherms predicted by the turbulence models considered in the present study. There exist only weak interactions between the two boundary layers near the hot and cold walls and a rotating core. The width of the cavity is large enough to establish separate boundary layers at the hot and cold walls and the core of the cavity is quiescent and thermally stratified. The isotherms predicted by the V2-f and SMC-PH models are equally spaced, while those by the two-layer and SST model are not equally spaced, indicating that the vertical centerline temperature distribution is not linear. There exists a small gradient of the temperature across the horizontal direction at the center region of the cavity in the prediction of the two-layer model, while the temperature distributions at the center region are nearly flat in the predictions of the V2-f and SMC-PH models. The temperature distribution predicted by the SMC-PH model near the top and bottom adiabatic walls are somewhat different from those by the other models. This kind of temperature distribution near the adiabatic walls was observed first in the computation by Dol and Hanjalic (2001) (see Fig. 2-(b) of their paper). They explain that

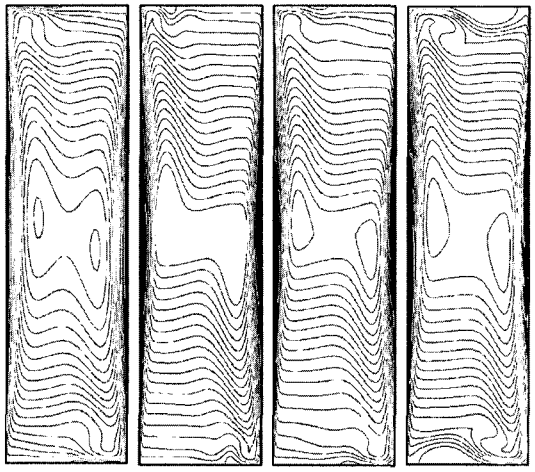

(a) Two-layer (b) SST (c) $\overline{v^2}-f$ (d) SMC-PH

Fig. 9 Streamlines predicted by four different turbulence molels

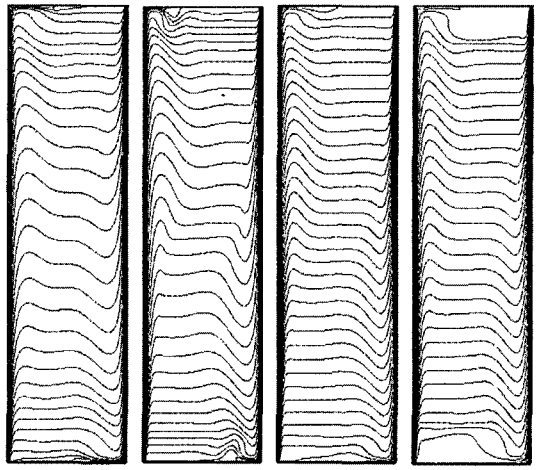

(a) Two-layer (b) SST (c) $\overline{v^2}-f$ (d) SMC-PH

Fig. 10 Isotherms predicted by four different turbulence molels

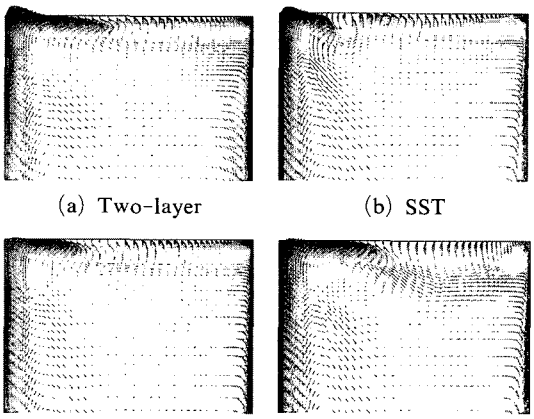

(a) Two-layer (b) SST

(c) $\overline{v^2}-f$ (d) SMC-PH

Fig. 11 Predicted velocity vector near the top wall by four diffrent turbulence models

the DNS data of Janssen (1994) and the experimental data by Opstelten (1994) support qualitatively this kind of temperature distribution by the SMC-PH model. Fig. 11 shows the predicted velocity vector near the top wall and it clearly shows why the streamlines and isotherms look like Fig. 9 and Fig. 10 near the top wall.

We first compare the predicted results with the measured data reported in Cheesewright et al. (1986) for the vertical mean velocity and the vertical velocity fluctuation at the mid-height ($y/H=0.5$) of the cavity. Figs. 12 (a)-(b) show the comparisons of the predicted results with the measured data for the vertical velocity component at $y/H=0.5$. As shown in the figures, the agreement between the measured data and the predictions by the V2-f and SMC-PH models is very good although there exists a small difference, and the two-layer model poorly predicts it. The SST model also predicts well the mean vertical velocity component. The two-layer model produces a laminar-like solution for the vertical velocity component in the near wall region. Choi et al. (2004) showed that the laminar-like solution produced by the two-layer model is due to the imposition of a smaller value of the turbulent eddy viscosity near the wall, indicating that the length scales in the two-layer model which is based on the forced convection flow should be modified for a natural convection flow. Fig. 13 shows the comparison of the predicted vertical velocity fluctuation at the mid-height ($y/H=0.5$) with the experimental data. It is shown that the V2-f and SMC-PH models predict properly the vertical velocity fluctuation when compared with the measured data. The SMC-PH model slightly over-predicts it and the V2-f model slightly under-predicts it in the near wall region. It is noted that the predictions by the V2-f and SMC-PH models generally follow the trend of the measured data. The two-layer model slightly under-predicts it in the near wall region and over-predicts it at the

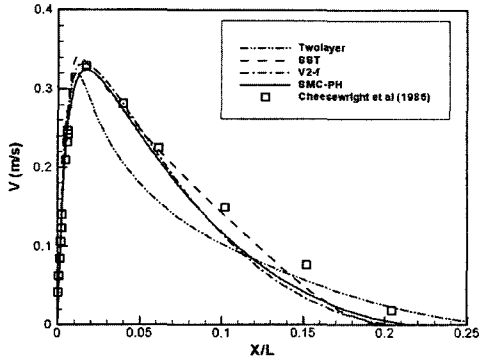

(a) Vertical velocity profiles

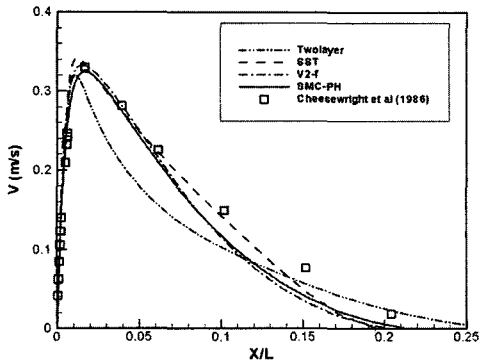

(b) Vertical velocity profiles close to the hot wall

Fig. 12 Mean vertical velocity profiles at $y/H=0.5$

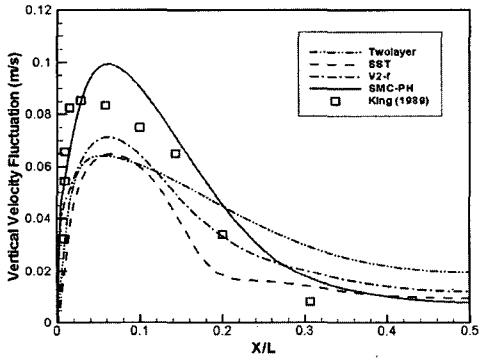

Fig. 13 Vertical velocity fluctuation profiles at $y/H=0.5$

edge of the boundary layer. This is due to the fact that the flow from the edge of the boundary layer to the core is quiescent and thermally stratified and the conventional $k-\varepsilon$ model, which can not handle properly the low level turbulence, is used to compute the flow and thermal fields in this region in the two-layer model. The SST model also predicts well the vertical velocity fluctuation,

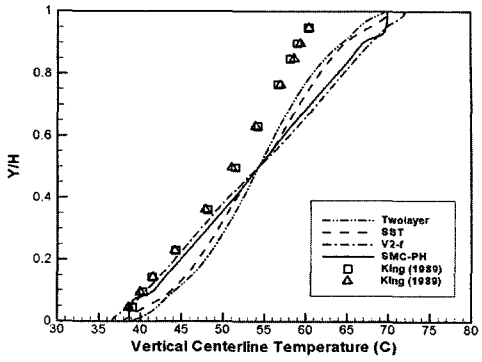

Fig. 14 Vertical centerline temperature profiles at $x/L=0.5$

but it predicts a little strange abrupt change at the edge of the boundary layer and the predicted profile is not smooth as shown in the predictions by the V2-f and SMC-PH models.

Figure 14 shows the comparison of the predicted vertical centerline temperature profiles at $x/L=0.5$ with the measured data by King (1989). We first note that the measured data of the vertical centerline temperature does not show the linear variation, and Cheesewright et al. (1986) explain that this phenomenon is due to the insufficient insulation of the side and upper walls. The heat loss from the side and upper walls causes the reduction of the temperature, and the centerline temperature deviates from the linear variation at the upper region of the cavity. The predicted results by the V2-f and SMC-PH models clearly exhibit the linear variation while the predictions by the two-layer and SST models do not show such a trend. The differences between the measured data with the predictions by the V2-f and SMC-PH models are believed to be due to the insufficient insulation of the side and upper walls, however, the predictions by the V2-f and SMC-PH models at the lower region of the cavity agree well with the measured data.

Figure 15 shows the profiles of the predicted Reynolds shear stress $\overline{uv}$ at the mid-plane ($y/H=0.5$) of the cavity together with the measured data. The SMC-PH and V2-f models predict well the $\overline{uv}$ profile near the hot wall, however, there exists a small difference between the measured data and the predicted results near the edge of the

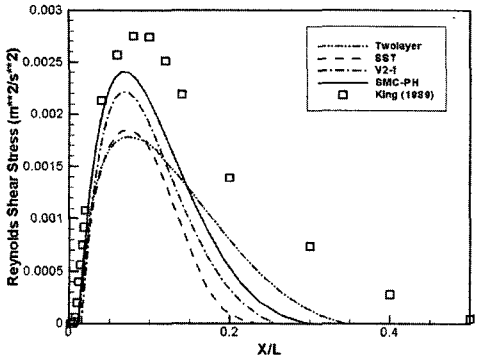

Fig. 15 Turbulent shear $\overline{uv}$ profiles at $y/H=0.5$

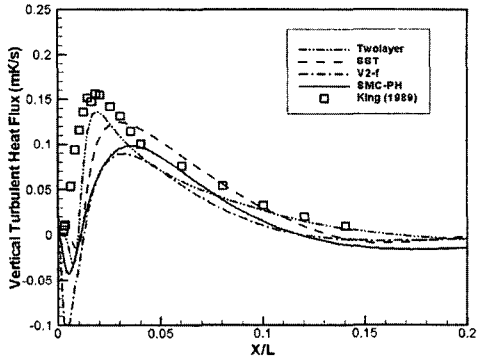

(a) Vertical turbulent heat flux $\overline{\theta v}$

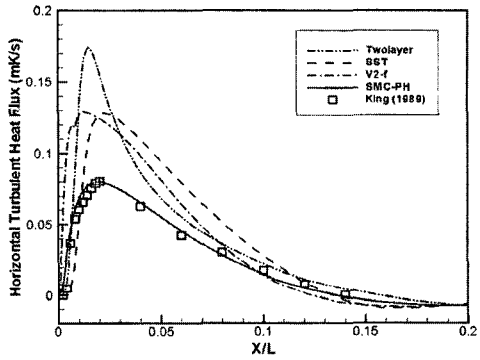

(b) Horizontal turbulence heat flux $\overline{\theta u}$

Fig. 16 Turbulent heat fluxes profiles at $y/H=0.5$

boundary layer. The two-layer and SST models under-predict the $\overline{uv}$ near the hot wall, however, the prediction by the SST model follows the trend of the experimental data. The two-layer predicts a rather diffusive profile at the edge of the boundary layer which is already observed in the predicted result for the vertical velocity fluctuation shown in Fig. 13. It is interesting to note that the predictions of the turbulent quantities by Kenjeres (1998) show a similar trend as the present prediction by the two-layer model, while the benchmark prediction reported in Henkes and Hoogendoorn (1995) follows the trend of the predictions by the V2-f and SMC-PH models.

Figures 16 (a)-(b) show the profiles of the predicted turbulent heat fluxes, $\overline{\theta v}$ and $\overline{\theta u}$, at the mid-plane ($y/H=0.5$) of the cavity with the measured data. It is noted that the vertical turbulent heat flux vector $\overline{\theta v}$ plays a very important role in the dynamics of the turbulent kinetic energy in the buoyant turbulent flows and influences directly the overall prediction of all the quantities. The AFM used in the present study, Eq. (9), for the two-layer, SST and V2-f models contains all the temperature and mean velocity gradients together with the correlation between the gravity vector and temperature variance. All the models predict well the vertical turbulent heat flux and this is due to the fact that the constant in the AFM have been adjusted to predict accurately the vertical turbulent heat flux. The V2-f and SMC-PH models slightly under-predict the turbulent heat flux $\overline{\theta v}$ near the hot wall and the peak regions of $\overline{\theta v}$ are skewed a little toward the center region as shown in Fig. 16-(a). The prediction by the SST model also follows well the general trend of the measured data. The two-layer model predicts well the vertical turbulent heat flux near the hot wall region and the peak regions are skewed to the hot wall, but the shape of the predicted profile is a little thin when compared with other predictions. Fig. 16-(b) shows that only the SMC-PH model predicts well the horizontal turbulent heat flux $\overline{\theta u}$ while the other models over-predict it. It shows that the AFM used in the present study needs some modifications. It is noted that the horizontal turbulent heat flux does not affect much the solution in the present test problem.

Figure 17 shows the comparison of the predicted results with the measured data for the wall shear stress at the hot wall reported in King (1989). We observe that the V2-f model predicts well the peak value of the wall shear stress at the hot wall, but it over-predicts the wall shear stress

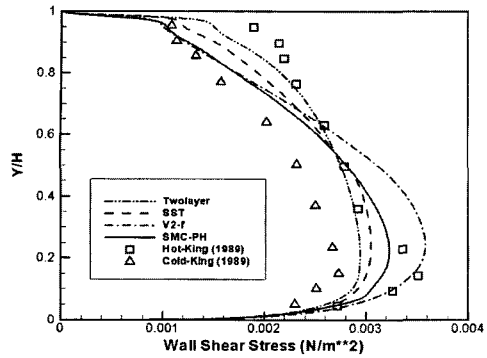

Fig. 17 Wall shear stress distributions along the hot wall

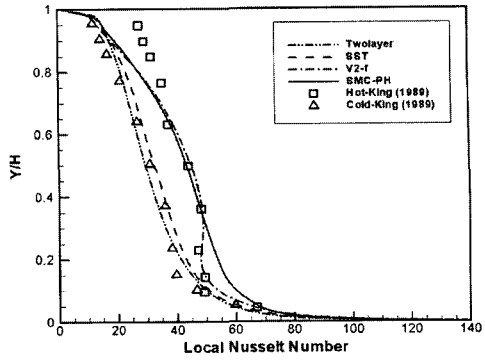

Fig. 18 Local Nusselt number distributions along the hot wall.

after the peak region. The general trend of the prediction of the wall shear stress by the SMC-PH model is the same as the V2-f model and the SMC-PH model slightly under-predicts the peak value of the wall shear stress. The general trend of the predictions by the two-layer and SST models is different from that by the V2-f and SMC-PH models. It is noted that the prediction by Kenjeres (1998) is very similar to the present predictions by the V2-f and SMC-PH models. We can observe that even the V2-f and SMC-PH models do not predict well the laminar to turbulent transition at the hot wall observed in the experimental data. They predict a smooth transition. It is quite interesting to note that the predictions of the vertical mean velocity by the V2-f and SMC-PH models agree well with the measured data as shown in Figs. 12 (a)-(b), but the predictions of the wall shear stress at a mid height of the cavity (y/H=0.3-0.5) are not satisfactory. Kenjeres (1998) explains that the experimental difficulties and uncertainties in measuring the velocity very close to the wall are most probably one of the reasons for the disagreement. Another source of disagreement can be the heat losses at the top of the cavity, which can cause a deformation of the velocity profile along the upper region.

Figure 18 shows the comparison of the predicted results with the measured data for the local Nusselt number at the hot wall reported in King (1989). The heat transfer coefficient reported in King (1989) is based on the centerline temperature as follows;

$$h_H(\Theta_H-\Theta_\infty)=-k_f\frac{\partial\Theta}{\partial x}\bigg|_{Hot\ Wall} \tag{18}$$

where h_H is the heat transfer coefficient at the hot wall, k_f is the thermal conductivity of the fluid and Θ_∞ is the temperature at the centerline (x/L=0.5). The local Nusselt number given in Fig. 18 is based on the temperature difference between the hot and cold walls. Thus, some manipulations are made using the experimental data of the centerline temperature given in Fig. 14. As explained above, the measured data of the centerline temperature do not exhibit the linear variation due to an insufficient insulation and this may affect the heat transfer coefficient. The V2-f model predicts accurately the local Nusselt number at the hot wall, and the transition phenomenon at the lower portion of the hot wall is also predicted well. The SMC-PH model also predicts well the local Nusselt number at the hot wall, however, it does not predict the laminar to turbulent transition observed in the experimental data. The two-layer and SST models predict poorly the local Nusselt number at the hot wall. The two-layer and SST models also do not predict the transition phenomenon. Kenjeres (1998) under-predicts the local Nusselt number at the hot wall and the predicted transition is weak and delayed (y/H=0.26) when compared with the experimental data (y/H=0.1) and the present prediction by the V2-f model (y/H=0.12).

5. Conclusions

The SMC-PH model and three different turbu-

lence models such as the two-layer model, the SST model and the V2-f model, all with the algebraic heat flux model, are tested for a natural convection in a rectangular cavity with isothermal and adiabatic walls. The primary emphasis of the present study is placed on the evaluation of the SMC-PH model for a natural convection problem. The optimal constants in the algebraic flux model for the two-layer, SST and V2-f models are sought by a systematic numerical experiment. The performances of the turbulence models are investigated through a comparison with the available experimental data. The following conclusions may be drawn from the present study;

(1) The two-layer model predicts poorly the mean vertical velocity and turbulent quantities such as the turbulent stresses and the turbulent heat fluxes, thereby, the wall shear stress and the local Nusselt number. This model predicts the diffusive solutions near the edge of the boundary layer to the center region. The length scales in the two-layer model formulation, which are based on the forced convection flow, should be modified to improve the prediction for the natural convection flows.

(2) The overall performance of the SST model is slightly better than that of the two-layer model, and this model also under-predicts the local Nusselt number and the wall shear stress at the hot wall. But this model avoids the diffusive solutions near the edge of the boundary layer to the center region.

(3) The general performance of the V2-f model is as good as that of the SMC-PH model and predicts well the laminar to turbulent transition, however, this V2-f, SST and two-layer models over-predict the horizontal turbulent heat flux when used with the algebraic heat flux model.

(4) The SMC-PH model predicts well for nearly all the quantities considered in the present study. This model is numerically very stable and shows a good convergence. One drawback of this model is its implementation in the flows with a complex geometry since this model involves many the wall related parameters.

As a concluding remark, the general performances of the SMC-PH model are much better than the two-layer and SST models based on the algebraic flux model. The V2-f model based on the algebraic flux model shows a very similar performance to the SMC-PH model. The algebraic flux model works well for the present test problem, but the optimal values of the constants in the algebraic flux model depend on the turbulence model used and the flow conditions. Thus, a modification of the algebraic flux model is needed for a better prediction of the natural convection in an enclosure. The V2-f type model should be extended to thermal flows to avoid using the algebraic flux model. Such a work is shown in the literature recently by Shin et al. (2004).

Acknowledgement

This study has been supported by the Nuclear Research and Development Program of the Ministry of Science and Technology of Korea.

References

Ampofo, F. and Karayiannis, T. G., 2003, "Experimental Benchmark Data for Turbulent Natural Convection in an Air Filled Square Cavity," *Int. J. Heat Mass Transfer*, Vol. 46, pp. 3551~3572.

Betts, P. L. and Bokhari, I. H., 2000, "Experiments on Turbulent Natural Convection in an Enclosed Tall Cavity," *Int. J. Heat Fluid Flow*, Vol. 21, pp. 675~683.

Boudjemadi, R., Maupu, V., Laurence, D., Quere and P. Le., 1997, "Budgets of Turbulent Stresses and Fluxes in a Vertical Slot Natural Convection Flow at Rayleigh $Ra=10^5$ and 5.4×10^5," *Int. J. Heat Fluid Flow*, Vol. 18, pp. 70~79.

Cheesewright, R., King, K. J. and Ziai, S., 1986, "Experimental Data for the Validation of Computer Codes for the Prediction of Two-Dimensional Buoyant Cavity Flows," *Proceeding of ASME Meeting, HTD*, Vol. 60, pp. 75~81.

Chen, H. C. and Patel, V. C., 1988, "Near-Wall Turbulence Models for Complex Flows Including Separation," *AIAA J.*, Vol. 26, pp. 641~648.

Choi, S. K., 2003, "Evaluation of Turbulence

Models for Natural Convection," *KAERI Internal Report*, FS200-AR-01-R0-03, (in Korean).

Choi, S. K., Kim, E. K. and Kim, S. O., 2004, "Computation of Turbulent Natural Convection in a Rectangular Cavity with the $k-\varepsilon-\overline{v^2}-f$ Model," *Numer. Heat Transfer, Part B*, Vol. 45, pp. 159~179.

Davidson, L. 1990, "Calculation of the Turbulent Buoyancy-Driven Flow in a Rectangular Cavity Using an Efficient Solver and Two Different Low Reynolds Number $k-\varepsilon$ Turbulence Model," *Numer. Heat Transfer, Part A*, Vol. 18, pp. 129~147.

Dol, H. S. and Hanjalic, K., 2001, "Computational Study of Turbulent Natural Convection in a Side-Heated Near-Cubic Cnclosure at a High Rayleigh Number," *Int. J. Heat Mass Transfer*, Vol. 44, pp. 2323~2344.

Dol, H. S., Hanjalic, K. and Kenjeres, S., 1997, "A Comparative Assessment of the Second-Moment Differential and Algebraic Models in Turbulent Natural Convection," *Int. J. Heat Fluid Flow*, Vol. 18, pp. 4~14.

Dol, H. S. Opstelten and I. J., Hanjalic, K., 2000, "Turbulent Natural Convection in a Side-Heated Near-Cubic Enclosure : Experiments and Model Computations," *Technical report APTFR/00-02*, Thermal and Fluids Science Section, Department of Applied Physics, Delft University of Technology, Delft, The Netherlands.

Hanjalic, K., 2002, "One-Point Closure Models for Buoyancy-Driven Turbulent Flows," *Annu. Rev. Fluid Mech.* Vol. 34, pp. 321~347.

Henkes, R. A. W. M. and Hoodendoorn, C. J., 1995, "Comparison Exercise for Computations of Turbulent Natural Convection in Enclosures," *Numer. Heat Transfer, Part B*, Vol. 28, pp. 59~78.

Henkes, R. A. W. M., Van Der Vlugt and F. F. Hoodendoorn, C. J., 1991, "Natural-Convection Flow in a Square Cavity Calculated with Low-Reynolds-Number Turbulence Models," *Int. J. Heat Mass Transfer*, Vol. 34, pp. 377~388.

Hsieh, K. J. and Lien, F. S., 2004, "Numerical Modeling of Buoyancy-Driven Turbulent Flows in Enclosures," *Int. J. Heat Fluid Flow*, in press.

Ince, N. Z. and Launder, B. E., 1989, "On the Computation of Buoyancy-Driven Turbulent Flows in Rectangular Enclosures," *Int. J. Heat Fluid Flow*, Vol. 10, pp. 110~117.

Ince, N. Z. and Launder, B. E., 1995, "Three-Dimensional and Heat-Loss Effects on Turbulent Flow in a Nominally Two-Dimensional Cavity," *Int. J. Heat Fluid Flow*, Vol. 16, pp. 171~177.

Kenjeres, S., 1998, "*Numerical Modelling of Complex Buoyancy-Driven Flows*," Ph. D Thesis, Delft University of Technology, The Netherlands.

Kenjeres, S., and Hanjalic, K., 1995, "Prediction of Turbulent Thermal Convection in Concentric and Eccentric Annuli," *Int. J. Heat Fluid Flow*, Vol. 16, pp. 429~439.

King, K. J., 1989, "*Turbulent Natural Convection in Rectangular Air Cavities*," Ph. D Thesis, Queen Mary College, University of London, U. K.

Janssen, R. J. A., 1994, "*Instabilities in Natural-Convection flows in Cavities*," Ph. D thesis, Delft University of Technology, Delft, The Netherlands.

Lai, Y. G., and So, R. M. C., 1990, "Near-Wall Modeling of Turbulent Heat Fluxes," *Int. J. Heat Mass Transfer*, Vol. 33, pp. 1429~1440.

Launder, B. E. and Sharma, B. I., 1974, "Application of the Energy Dissipation Model of Turbulence to the Calculation of Flow Near Spinning Disc," *Lett. In Heat and Mass Transfer*, Vol. 1, pp. 131~138.

Lien, F. S., and Leschziner, M. A., 1991, "Second-Moment Modelling of Recirculating Flow with a Non-orthogonal Collocated Finite-Volume Algorithm," *Turbulent Shear Flows*, Vol. 8, pp. 205~222.

Medic, G. and Durbin, P. A., 2002, "Toward Improved Prediction of Heat Transfer on Turbine Blades," *J. Turbomachinery*, Vol. 124, pp. 187~192.

Menter, F. R., 1994, "Two-Equation Eddy-Viscosity Turbulence Models for Engineering Applications," *AIAA Journal*, Vol. 32, No. 8, pp. 1598~1604.

Opstelten, I. J., 1994, "*Experimental Study on Transition Characteristics of Natural-Convection Flow*," Ph. D thesis, Delft University of Technology, Delft, The Netherlands.

Patankar, S. V., 1980, "*Numerical Heat Transfer and Fluid Flow*," Hemisphere, New York, USA.

Peeters, T. W. J. and Henkes, R. A. W. M., 1992, "The Reynolds-Stress Model of Turbulence Applied to the Natural-Convection Boundary Layer along a Heated Vertical Plate," *Int. J. Heat Mass Transfer*, Vol. 35, pp. 403~420.

Peng, S. H. and Davidson, L., 2001, "Large Eddy Simulation of Turbulent Buoyant Flow in a Confined Cavity," *Int. J. Heat Fluid Flow*, Vol. 22, pp. 323~331.

Shikazo, N. and Kasagi, N., 1996, "Second Moment Closure for Turbulent Scalar Transport at Various Prandtl Numbers," *Int. J. Heat Mass Transfer*, Vol. 39, pp. 2977~2987.

Shin, J. K., An, J. S. and Choi, Y. D. 2004, "Near Wall Modelling of Turbulent Heat Fluxes by Elliptic Equation." *Transactions of the Korean Society of Mechanical Engineers, Part B*. Vol. 28, pp. 526~534.

Shin, J. K., Choi, Y. D. and Lee, G. H., 1993, "A Low-reynolds Number Second Moment Closure for Turbulent Heat Fluxes," *Transactions of the Korean Society of Mechanical Engineers, Part B*. Vol. 17, pp. 3196~3207.

Tian, Y. S. and Karayiannis T. G., 2000, "Low Turbulence Natural Convection in an Air Filled Square Cavity part I: The Thermal and Fluid Flow Fields," *Int. J. Heat Mass Transfer*, Vol. 43, pp. 849~866.

Tieszen, S., Ooi, P., Durbin, P. A. and Behnia, M., 1998, "Modeling of Natural Convection Heat Transfer," *Proc. Summer Program*, Center of Turbulence Research, Stanford University, Stanford, CA, U. S. A., pp. 287~302.

Tsuji, T and Nagano, Y., 1987, "Turbulence Measurements in a Natural Convection Boundary Layer along a Vertical Flat Plate," *Int. J. Heat Mass Transfer*, Vol. 31, pp. 2101~2111.

Van Leer, B., 1974, "Towards the Ultimate Conservative Difference Scheme: Monotonicity and Conservation Combined in a Second Order Scheme," *J. Comput. Phy.*, Vol. 14, pp. 361~370.

Versteegh, T.A.M. and Nieuwstat, F.T.M., 1998, "Turbulence Budgets of Natural Convection in an Infinite, Differentially Heated, Vertical Wall," *Int. J. Heat Fluid Flow*, Vol. 19, pp. 135~149.

Zhu, J., 1991, "A Low-Diffusive and Oscillation Free Convection Scheme," *Comm. Appl. Numer. Methods*, Vol. 7, pp. 225~232.

Appendix

$$P_{ij}=-\rho\left(\overline{u_iu_k}\frac{\partial U_j}{\partial x_k}+\overline{u_ju_k}\frac{\partial U_i}{\partial x_k}\right),\quad P_k=\frac{1}{2}P_{kk}$$

$$G_{ij}=-\rho\beta(g_i\overline{\theta u_j}+g_j\overline{\theta u_i}),\quad G_k=\frac{1}{2}G_{kk}$$

$$\varepsilon_{ij}=(1-f_s)\frac{2}{3}\varepsilon\delta_{ij}+f_s\frac{\varepsilon}{k}\overline{u_iu_j},\quad f_s=\frac{1}{1+R_T/10},\quad R_T=\frac{k^2}{\nu\varepsilon}$$

$$E_{ij}=\begin{cases}-2\mu\dfrac{\overline{u_iu_j}}{x_n^2}, & i=j\\[2ex] -2\mu\dfrac{\overline{u_iu_j}+\overline{u_iu_k}n_kn_j+\overline{u_ju_k}n_kn_i+\overline{u_ku_l}n_kn_in_in_j}{x_n^2}, & i\neq j\end{cases}$$

$$E_\varepsilon=-2\mu\frac{\varepsilon}{x_n^2}\exp(-0.5x_n^+),\qquad x_n^+=\frac{\rho U_\tau x_n}{\mu},\qquad U_\tau=\left(\frac{\mu}{\rho}\left|\frac{\partial U_P}{\partial x_n}\right|_w\right)^{1/2}$$

$$\Phi_{ij}=\Phi_{ij1}+\Phi_{ij2}+\Phi_{ij3}+\Phi_{ijw1}+\Phi_{ijw2}$$

$$\Phi_{ij1}=-C_1\rho\frac{\varepsilon}{k}\left(\overline{u_iu_j}-\frac{2}{3}k\delta_{ij}\right),$$

$$\Phi_{ij2}=-C_2\left(P_{ij}-\frac{2}{3}P_k\delta_{ij}\right),$$

$$\Phi_{ij3}=-C_3\left(G_{ij}-\frac{2}{3}G_k\delta_{ij}\right)$$

$$\Phi_{ijw1}=-\rho C_{w1}\frac{\varepsilon}{k}\left(\overline{u_ku_m}n_kn_m\delta_{ij}-\frac{3}{2}\overline{u_ku_i}n_kn_j-\frac{3}{2}\overline{u_ku_j}n_kn_i\right)\frac{k^{3/2}}{C_l\varepsilon\Delta n}$$

$$\Phi_{ijw2}=-C_{w2}\left(\Phi_{km2}n_kn_m\delta_{ij}-\frac{3}{2}\Phi_{ik2}n_kn_j-\frac{3}{2}\Phi_{jk2}n_kn_i\right)\frac{k^{3/2}}{C_l\varepsilon\Delta n}$$

$$P_{i\theta}^t=-\rho\overline{u_iu_k}\frac{\partial\Theta}{\partial x_k},\quad P_{i\theta}^m=-\rho\,\overline{\theta u_k}\frac{\partial U_i}{\partial x_k},\quad G_{i\theta}=-\rho\beta g_i\overline{\theta^2},$$

$$P_\theta=-\rho\overline{\theta u_k}\frac{\partial\Theta}{\partial x_k},\quad E_{i\theta}=-\left(\frac{\mu}{\mathrm{Pr}}+\mu\right)\frac{\overline{\theta u_i}+\overline{\theta u_k}n_kn_i}{x_n^2},\quad E_\theta=-2\frac{\mu}{\mathrm{Pr}}\frac{\overline{\theta^2}}{x_n^2}$$

$$\Phi_{i\theta}=\Phi_{i\theta1}+\Phi_{i\theta2}+\Phi_{i\theta3}+\Phi_{i\theta w}$$

$$\Phi_{i\theta1}=-C_{\theta1}\rho\frac{\varepsilon}{k}\overline{\theta u_i},$$

$$\Phi_{i\theta2}=-C_{\theta2}P_{i\theta}^m,$$

$$\Phi_{i\theta3}=-C_{\theta3}G_{i\theta}$$

$$\Phi_{i\theta w}=C_{\theta w}\Phi_{k\theta1}n_kn_i\frac{k^{3/2}}{C_l\varepsilon\Delta n}$$

$$f_{\varepsilon1}=1,\ f_{\varepsilon2}=1.\ -\frac{2}{9}\exp\left[-\left(\frac{R_T}{6}\right)^2\right]$$

$$C_s=0.20,\ C_\varepsilon=0.15,\ C_{\theta u}=0.20,\ C_{\theta\theta}=0.22,\ C_{\varepsilon\theta}=0.22$$

$$C_{\varepsilon1}=1.35,\ C_{\varepsilon2}=1.80,\ C_{\varepsilon3}=1$$

$$C_1=2.2,\ C_2=0.55,\ C_3=0.55,\ C_{w1}=0.6,\ C_{w2}=0.3,\ C_l=2.53$$

$$C_{\theta1}=3.75,\ C_{\theta2}=0.5,\ C_{\theta3}=0.5,\ C_{\theta w}=0.2$$

$$C_{P1}=1.8,\ C_{P2}=0.72,\ C_{D1}=2.2,\ C_{D2}=0.8$$